Numerical study of an oscillating cylinder in uniform flow and in the wake of an upstream cylinder

By JING LI[1], JIONG SUN[2] AND BERNARD ROUX[1]

[1] Institut de Mécanique des Fluides de Marseille-CNRS UM34, 1 Rue Honnorat,
13003 Marseille, France

[2] Laboratoire de Recherche en Combustion, Université d'Aix-Marseille I, Centre de St-Jérôme,
Case 252, Avenue Escadrille Normandie Niemen, 13397 Marseille Cedex 13, France

Direct numerical simulation is carried out to study the response of an oscillating cylinder in uniform flow and in the wake of an upstream cylinder. It is found that the response of the cylinder wake is either a periodic (lock-in) or a quasi-periodic (non-lock-in) state. In the lock-in state, the vortex shedding frequency equals the forcing frequency. In the non-lock-in state, the shedding frequency shows a smooth variation with the driving frequency. For a cylinder oscillating in uniform flow, a lock-in diagram of different forcing amplitude is computed. However, no clear chaotic behaviour is detected near the lock-in boundary. For a cylinder oscillating in the wake of an upstream cylinder, the response state is strongly influenced by the distance between the two cylinders. By changing cylinder spacing, two different flow regimes are identified. In the 'vortex formation regime', found at large spacings, the vortex street develops behind both the upstream and downstream cylinders. The strength of the naturally produced oscillation upstream of the second cylinder becomes important compared to the forced oscillation and dominates the flow, leading to a very small or even indistinguishable zone of synchronization. However, in the 'vortex suppression regime', observed at small spacings, the oncoming flow to the downstream cylinder becomes so weak that it hardly affects its vortex wake, and therefore a large zone of synchronization is obtained. The numerical results are in good agreement with available experimental data.

1. Introduction

The investigation of vibrating cylinder–vortex wake interaction is of great importance not only as a basic problem in fluid mechanics but also for flow-control problems in engineering applications.

The response in the wake of a circular cylinder oscillating in uniform flow has been intensively studied experimentally. The vibrating cylinder–vortex wake system is known to produce many interesting effects characteristic of a nonlinear self-excited oscillator (Berger & Wille 1972), such as the lock-in phenomena which was first reported by Bishop & Hassan (1964). According to their observations, when the forcing frequency approaches the vortex shedding frequency, the natural Strouhal frequency is suppressed by the cylinder vibration frequency. This phenomena also occurs when the forcing frequency is a multiple or submultiple of the natural vortex shedding frequency. Additional experimental results on the behaviour of vortex

shedding in the presence of external forcing are found in, for example, Koopmann (1967), Berger & Wille (1972), Griffin & Ramberg (1975), Bearman (1984). The influence of the cylinder vibration during synchronization can be summarized as: (i) it increases the vortex strength; (ii) it replaces slantwise vortex shedding with parallel vortex shedding; (iii) it synchronizes the vortex shedding frequency to the forcing frequency; (iv) and finally, it increases the force acting on the cylinder (Blevins 1977).

There has been increasing interest during the last decade in the investigation of the laminar wake of cylinders to reveal the origin of the discontinuity in the relation between the Strouhal number (non-dimensional vortex shedding frequency) and the Reynolds number first observed by Tritton (1959, 1971). Based on his experimental observations, Gaster (1969, 1971) suggested that the discontinuity was possibly caused by flow non-uniformity. Sreenivasan (1985) observed that as the Reynolds number was increased, the initial vortex shedding state with a single shedding frequency was replaced by a two-frequency-quasi-periodic state. This 'ordered' behaviour persisted until the appearance of 'a window of chaos' over a small range of Re, where the discontinuous variation of Strouhal number with Re was detected. Sreenivasan believed that such chaotic patterns could develop even at low Reynolds numbers, for which flow is still laminar. With regard to this question, Van Atta & Gharib (1987) investigated the wake of a vibrating wire and suggested that the 'window of chaos' observed by Sreenivasan was not of pure fluid-mechanical origin, but was in fact due to aeroelastic coupling of the vortex wake with cylinder vibration modes. These authors suggested that this competitive coupling between the naturally produced vortex wake and the forced cylinder vibration was responsible for the discontinuity in the Strouhal–Reynolds number relation reported by Tritton. Following Van Atta & Gharib's work, Karniadakis & Triantafyllou (1989) carried out a two-dimensional numerical simulation. By exerting an external forcing, which is harmonic in time and localized in space, in the near wake of the cylinder, they studied the frequency selection process and the asymptotic states in the laminar wake of a circular cylinder and demonstrated that the possible asymptotic response states of a forced wake could be periodic or quasi-periodic depending on the combination of the amplitude and frequency of the external forcing. They also demonstrated that chaotic states could be created by external forcing.

On the other hand, Williamson (1989) showed that, even in the absence of cylinder vibration and flow non-uniformity, a discontinuity in the St–Re relation could still exist due to a three-dimensional flow mode transition (from one oblique shedding mode to another oblique mode). The phenomenon of oblique shedding was found to be caused by end effects. Williamson observed that, by manipulating the end boundary conditions, parallel shedding could be produced (which can be regarded as a two-dimensional flow), resulting in a completely continuous St–Re curve. He further demonstrated that the parallel shedding Strouhal curve is universal: if one considers normally directed oblique shedding, one can find the same curve as the parallel shedding Strouhal curve. Based on the similarity of oblique shedding angles between his experimental data and those derived from Tritton's measurements, Williamson showed that Tritton's discontinuity was possibly caused by the breakdown of one oblique shedding mode to another. However, Williamson's three-dimensionally originated discontinuity is found to occur at $Re = 64$, which is not very close to the value where Tritton found his discontinuity ($Re \approx 90$). The reason for this difference is not clear, though the flow non-uniformity, the turbulence level, the end conditions and the vibration of the cylinder may be responsible.

In engineering applications, flow-induced vibration is often inevitable. This can alter the frequency and the intensity of the forces acting on a structure as well as vortex wake characteristics. In this paper, we focus on the two-dimensional aspects of the interaction between forced cylinder vibration and its vortex wake. However it should be born in mind that three-dimensional effects can be important in some cases, e.g. the oblique vortex shedding mode transition studied by Williamson (1989).

Even in the two-dimensional case, the analytical solution of such problems is very difficult, since the solution of such nonlinear PDEs is not currently available. Therefore, the numerical methods have been proposed in the last few decades. Besides the work of Karniadakis & Triantafyllou cited above, which emphasized the frequency selections, other numerical studies on various characteristics of the lock-in state have been undertaken. Chilukuri (1987) developed an implicit finite-difference scheme to investigate the vortex shedding characteristics behind a transversely vibrating cylinder subjected to uniform flow. The coordinate system was transformed to the oscillating cylinder frame, converting the uniform free-stream boundary conditions to oscillatory ones. His numerical results showed good agreement with experimental data for small vibration amplitude. The same problem was also treated by Anagnostopoulos (1989), who used the stream function–vorticity formulation. For each time step, the grid system was displaced with the cylinder vibration to a new location, and the corresponding new velocity field was then computed for the newly displaced grid system.

Most previous investigators have emphasized the role of cylinder vibration; the influence of upstream disturbances on vortex shedding characteristics has been overlooked. In fact, interactions among the oscillating oncoming flow, the oscillating cylinder and the vortex wake are extremely important and occur frequently. Serious instabilities have been reported in arrays of tubes in heat exchangers, power cables, etc. Barbi *et al.* (1986) showed evidence of lock-in due to harmonic perturbation of the freestream velocity. The question remains: what will be the combined effect of the cylinder vibration and the oscillation of the oncoming flow, or in more physical sense, what is the dynamics of an oscillating cylinder in a wake of another cylinder? The investigation of such a nonlinear system is worthwhile because it can offer significant insight to the flow interactions and wake–cylinder vibration–wake coupling. Despite its importance, such a problem has not interested many investigators. The only documentation we can find in the literature is the experimental work of Tanida, Okajima & Watanabe (1973), in which the instability of two cylinders in a tandem configuration with downstream cylinder vibration was studied. The problem seems similar to that where an oscillating cylinder is placed in an harmonically oscillating flow; however, the flow configurations can be significantly different. In the case of two cylinders in tandem, the spacing between the two cylinders strongly affects the intensity of the oscillatory incident flow on the downstream cylinder. Moreover, there is a critical spacing separating two different flow configurations: the 'vortex suppression regime' and the 'vortex formation regime' (Ishigai *et al.* 1972; Zdravkovich 1977; Li 1989; Li *et al.* 1991). In the 'vortex suppression regime', two attached, almost symmetrical vortices are formed between the two cylinders, only very weak or even no oscillations can be detected behind the cylinders, at least in the near wake. In the 'vortex formation regime', vortices are shed normally from the upstream cylinder, creating oscillations in the flow upstream of the second cylinder. The changes in lock-in characteristics caused by the changes in flow configurations will be discussed in detail in §4.

The present work is a direct numerical simulation to study the response state of a circular cylinder oscillating in uniform flow and in the wake of an upstream cylinder. An exact formulation would account for the time displacement of the mesh system due to the oscillation of the cylinder. However, to simplify the analysis and the programming, as well as to save computation time we consider, instead of a really oscillating cylinder, a quiescent cylinder with a periodic parietal velocity (aspiration or transpiration through the wall). An investigation of the problem by taking into consideration the moving mesh system is underway; the first results have demonstrated the same qualitative behaviour as that to be described in the present paper. This further justifies the use of a periodic parietal velocity as a forcing mechanism.

The organization of the paper is as follows: §2, the numerical formulation employed is described; in §§3 and 4, the numerical results for a cylinder oscillating in uniform flow and in the wake of an upstream cylinder, respectively, are presented and compared with experimental data; and finally conclusions are drawn in §5.

2. Numerical formulation

We consider the flow to be laminar, incompressible and two-dimensional. The governing momentum equation and equation of mass conservation in dimensionless forms are

$$\frac{\partial \boldsymbol{u}}{\partial t} + \boldsymbol{u} \cdot \nabla \boldsymbol{u} = -\nabla p + \frac{1}{Re}\nabla^2 \boldsymbol{u} \qquad (1)$$

$$\nabla \cdot \boldsymbol{u} = 0, \qquad (2)$$

where $\boldsymbol{u}$ is the velocity vector with components u and v in the x- and y-directions, respectively, $Re = U_\infty D/\nu$ is the Reynolds number, with U_∞ the free-stream velocity, D the cylinder diameter and ν the kinematic viscosity of the fluid.

The computational domain and boundary conditions for the two-cylinder model are depicted in figure 1. The boundary conditions for inlet, upper and lower boundaries are: $u = 1$, $v = 0$, whereas natural boundary conditions: $\sigma_{ij} n_j = 0$ are chosen for the outflow boundary, with

$$\sigma_{ij} = -p\delta_{ij} + \frac{1}{Re}\left(\frac{\partial u_i}{\partial x_j} + \frac{\partial u_j}{\partial x_i}\right). \qquad (3)$$

The influence of the outflow boundary on vortex shedding characteristics is discussed in the benchmark solution of Engelman & Jamnia (1990). It was found that even for a distance from the cylinder centre to the outflow boundary as small as $4D$, the discrepancy with the benchmark solution was less than 15%. This shows that the natural outlet boundary condition is well suited to vortex shedding problems. In our simulation, this distance is $20D$ (comparable to $25D$ used in the benchmark solution), so the influence of the outflow boundary is negligible.

For the fixed cylinder, $u = 0$, and $v = 0$ are imposed on the cylinder surface whereas for oscillating cylinder, the following boundary conditions are adopted:

$$u = 0, \qquad v(t) = A_v \sin(2\pi f_c t), \qquad (4)$$

where f_c is the forcing frequency and A_v, the parietal velocity amplitude. For a vibrating impervious cylinder, A_v is related to the displacement amplitude A by the relation: $A_v = 2\pi f_c A$. In our case, A is considered as a fictitious displacement amplitude.
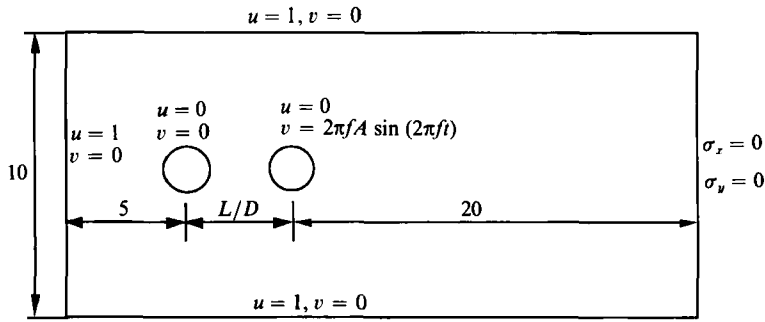
FIGURE 1. Computational domain and boundary conditions of the two-cylinder model.
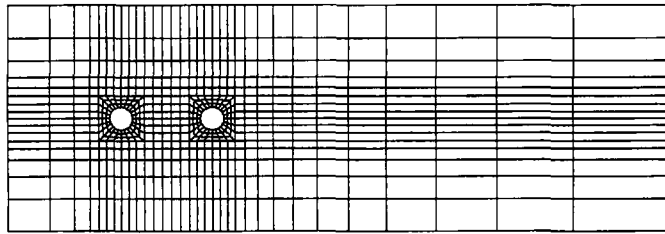

FIGURE 2. A typical mesh for the two-cylinder model (584 elements and 2479 nodes).

A complete description of the numerical technique employed can be found in our previous studies on vortex shedding from cylinders (Li 1989; Li *et al.* 1991). Only a brief overview of the approach employed in the present paper will be presented here. The time-dependent Navier–Stokes equations are solved in their primitive variable form. Nine-node quadrilateral elements are used with a biquadratic Lagrange interpolation function for the velocities and a bilinear interpolation function for the pressure. The transient time integration is performed using the second-order, non-dissipative and completely stable Crank–Nicolson time integrator. The nonlinear algebraic system was solved using Newton–Raphson iteration. In addition to the primary velocity and pressure variables, we also calculate the drag and lift forces exerted on the cylinder from the following formulae:

$$C_d = 2 \oint_{\text{cylinder}} \left\{ -p\,\mathrm{d}x + \frac{1}{Re}\left[2\frac{\partial u}{\partial x}\,\mathrm{d}x + \left(\frac{\partial u}{\partial y}+\frac{\partial v}{\partial x}\right)\mathrm{d}y\right]\right\},$$

$$C_l = 2 \oint_{\text{cylinder}} \left\{ -p\,\mathrm{d}y + \frac{1}{Re}\left[\left(\frac{\partial u}{\partial y}+\frac{\partial v}{\partial x}\right)\mathrm{d}x + 2\frac{\partial v}{\partial y}\,\mathrm{d}y\right]\right\}.$$

A variable finite-element grid is used with finer mesh close to the cylinder and coarser elements further downstream. An example of the two-cylinder model is given in figure 2. The program has been tested for fixed cylinders as in our previous studies (Li 1989; Li *et al.* 1991). In order to demonstrate the consistency of our solutions in a mesh refinement sense for both a fixed and an oscillatory cylinder, computations are also performed on a refined mesh (2598 nodes) which is approximately two times finer than the mesh usually used (1394 nodes). A comparison is made for the main flow characteristics with some existing experimental and numerical data for the fixed cylinder case, including the benchmark solution of Engelman & Jamnia (1990) (14000 nodes) (see table 1). Generally good agreement is observed except for an

	Strouhal number	Average drag coefficient	Lift coefficient peak-to-peak
Mesh used in present work (1394 nodes)	0.166	1.256	0.637
Finer mesh (2598 nodes)	0.176	1.333	0.685
Benchmark solution (14000 nodes) (Engelman & Jamnia (1990))	0.173	1.411	0.7267
Braza et al. (1986) (numerical simulation)	0.16	1.3	0.6
Tritton (1959) (experiments)	0.15–0.18	1.26–1.32	—

TABLE 1. Comparison of main flow characteristics with some experimental and numerical results $(Re = 100)$

underestimation of the lift coefficient. For the oscillatory cylinder case, no difference is found in shedding frequency; however, differences of 3 and 5% are observed in drag and lift coefficients, respectively.

In order to study the interactions between cylinder vibration and its periodic wake, the solutions of vortex shedding from fixed cylinders were first computed until the periodic vortex street was well established. This solution is then applied as initial condition for our forced vortex wake simulations. The amplitude of oscillation is kept constant whereas the forcing frequency is varied in order to localize the lock-in boundary. The response states in the cylinder wake are followed in time and the characteristic vortex shedding frequency is determined using power spectra and phase diagrams. In the case of two cylinders in tandem, by changing the cylinder spacings, different intensities of oscillation of the incident flow on the downstream cylinder can be introduced; the interactions among the cylinder vibration, its upstream oscillation and the downstream vortex wake are then studied. The computations were performed on an IBM 3090-VF computer, the average CPU time is about 30.7 s per time step for two-cylinder calculations; and on a Intel iPSC/860 computer, which is about 79.7 s per time step on a single processor (vectorizer being not yet available).

3. Results for one cylinder oscillating transversely in uniform flow

In this section, the response of the cylinder wake to cylinder oscillation is investigated in the case of uniform upstream flow. In the following, f_c is used to indicate cylinder oscillation frequency, f_s the vortex shedding frequency in the presence of cylinder oscillation, and f_{ns} the natural shedding frequency.

3.1. Lock-in and non-lock-in behaviour

By varying the forcing frequency, both a lock-in and a non-lock-in state have been observed in our numerical simulations.

When the frequency of external forcing applied on the cylinder is sufficiently close to the vortex shedding frequency, the vortex shedding frequency rapidly changes towards the driving frequency. This state is denoted the lock-in state, in which the power spectrum shows a dominant peak at the driving frequency f_c (figure 3). The drag and lift forces, as well as the longitudinal and the transverse velocities are periodic functions of time with constant amplitudes. The variation of drag and lift coefficients over time is plotted in figure 4. It is obvious that the effect of
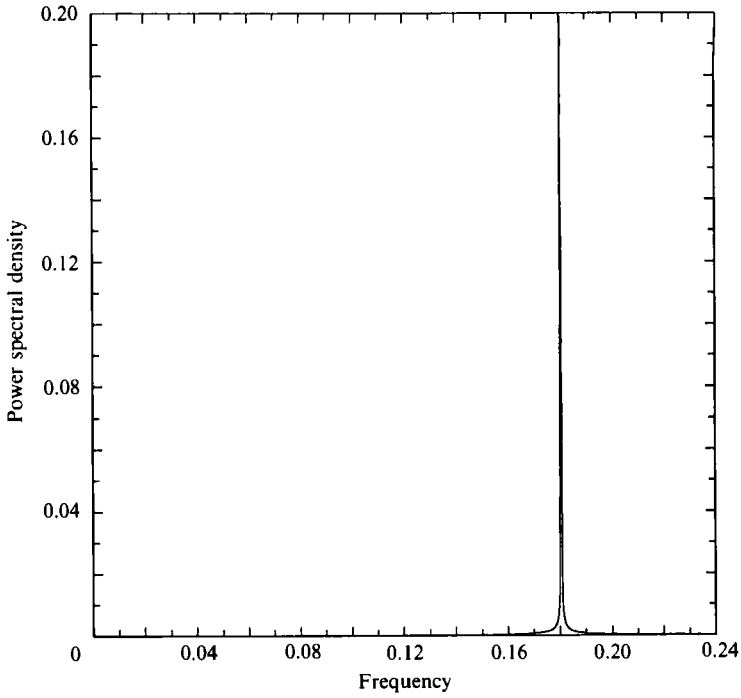
FIGURE 3. Power spectrum of the lock-in state ($Re = 100$, $A_v = 0.05$ and $f_c = 1.1f_{ns}$), with dominant frequency at the forcing frequency f_c.
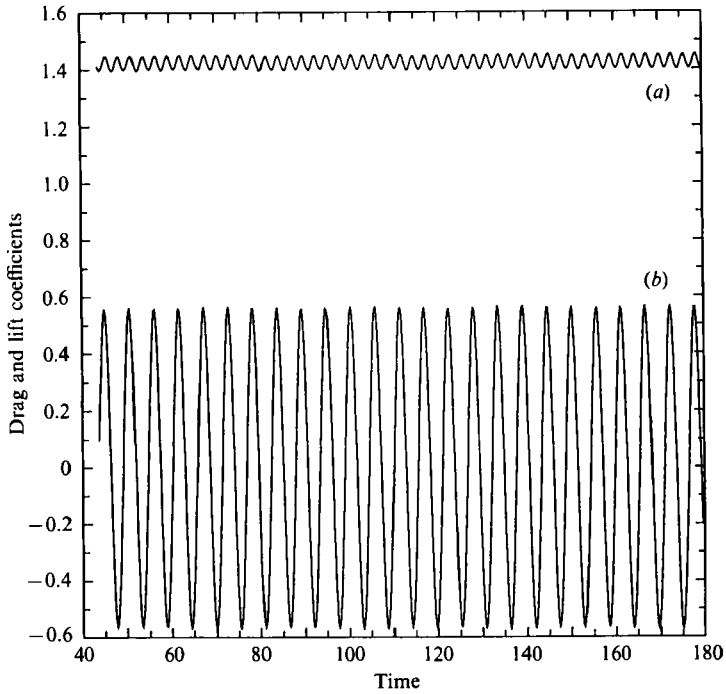

FIGURE 4. Time history of drag (curve a) and lift (curve b) coefficients in lock-in state, same conditions as in figure 3.
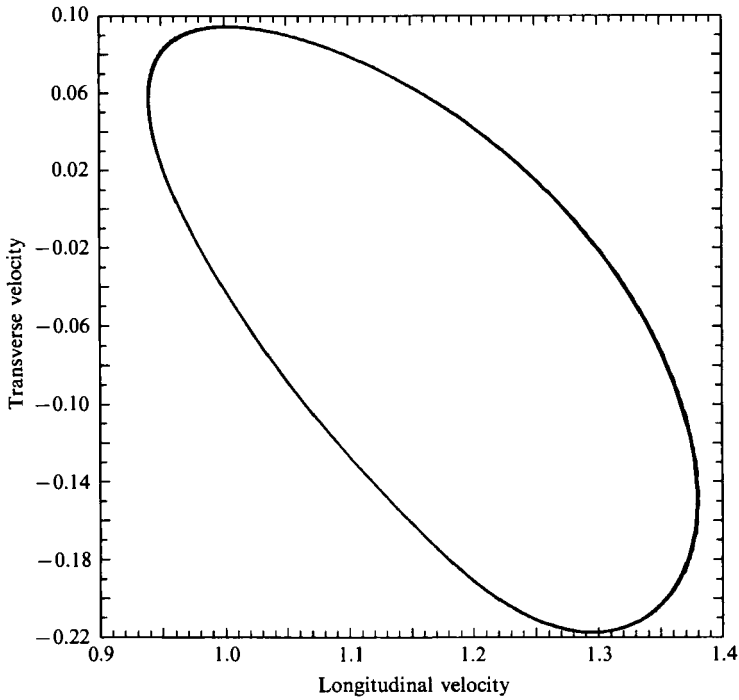
FIGURE 5. Phase diagram of the lock-in state, periodic response, velocities are taken at the point $x = 0.7828$, $y = 0.7828$; $A_v = 0.05$ and $f_c = 1.1f_{ns}$.
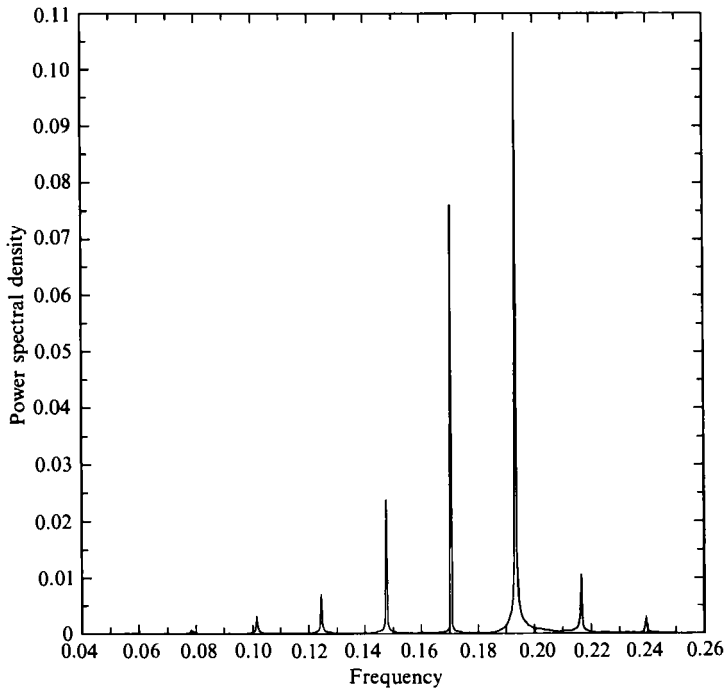

FIGURE 6. Power spectrum for non-lock-in state ($Re = 100$, $A_v = 0.05$ and $f_c = 1.18f_{ns}$), two dominant frequencies as well as their harmonics are observed. We note that the shedding frequency is not strictly equal to the natural shedding frequency, but has drifted towards the forcing frequency ($f_{ns} = 0.166$, $f_s = 0.171$).

'synchronization' or 'lock-in' is to stabilize the vortex wake. The periodicity of the vortex wake is also apparent in phase diagrams. This method has proved useful in analysing and identifying different response states in the wake of the cylinder (Koopmann 1967; Karniadakis & Triantafyllou 1989). To obtain phase diagrams, we chose two arbitrary independent variables of the system: longitudinal and transverse velocity components at the point $x = 0.7828$, $y = 0.7828$ in the near wake. A single loop is observed in a Lissajous figure as the lock-in state is reached (figure 5), showing a completely periodic trajectory representing a periodic vortex wake.

Outside the lock-in region, a quasi-periodic response state is obtained. Near the lock-in boundary, nonlinear interactions between the vortex street and the forced vibration become preponderant in determining the resulting state of the cylinder wake. We detected both forcing and shedding frequencies in the power spectra, but the latter is not strictly equal to the natural shedding frequency, it has drifted towards the forcing frequency (figure 6). Similar variation was observed experimentally by Barbi *et al.* (1986) in the wake of a stationary cylinder placed in longitudinally oscillating flow. We refer to this response state as an intermediate state (see also figure 10). The relative strengths of the frequencies depend on the comparative importance of the waves generated by the vortex street and by the oscillation of the cylinder. Nonlinear interactions of the two waves result in composite wave forms of both the longitudinal and transverse velocities. The phase diagram is shown in figure 7; an aperiodic trajectory is found. For drag and lift forces, composite wave forms due to nonlinear interactions have also been observed. The time history of drag and lift coefficients at $f_c = 1.18 f_{ns}$ is plotted in figure 8. Similar wave forms have been experimentally observed by Bishop & Hassan (1964) for the same problem of a mechanically vibrated cylinder outside its synchronization range.

When the forcing frequency is far from the natural shedding frequency, a typical non-lock-in state is observed. The power spectrum exhibits two peaks, one at the shedding frequency and the other at the forcing frequency. The two frequencies are also seen in the phase diagram (figure 9).

In the intermediate region, also referred as the 'receptivity region' in some literature, chaotic behaviour in the wake may develop as described by Karniadakis & Triantafyllou (1989). This chaotic behaviour is characterized by a sudden broadening of the spectrum and loss of periodicity in time signals. However, no clear chaotic behaviour was detected in our simulations. This may be attributed to several factors. First, whether a chaotic state really exists under the present forcing mechanism is not clear; different forcings may lead to different responses. Second, the precise identification of the chaotic response requires much longer time signals (at least for 150–200 stabilized vortex shedding periods) in order to obtain the reliable power spectra. Also, the reconstruction of time signals will be inadequate to identify the chaotic state, since the chaotic state is never repeatable; the reconstruction will introduce artificial frequencies indistinguishable from the real signal frequencies. Therefore it is computationally expensive to obtain such long time signals, and we did only a few such computations and did not capture apparent chaotic responses. On the other hand as, according to Karniadakis & Triantafyllou, the chaotic state can only be observed in a very narrow region, it is difficult to locate precisely in this region and in our simulation we might overlook it. Nevertheless, this is an interesting problem and worth further investigation since it can shed light on whether in the two-dimensional case, a general forcing mechanism on a cylinder or in a wake can lead to a chaotic response.
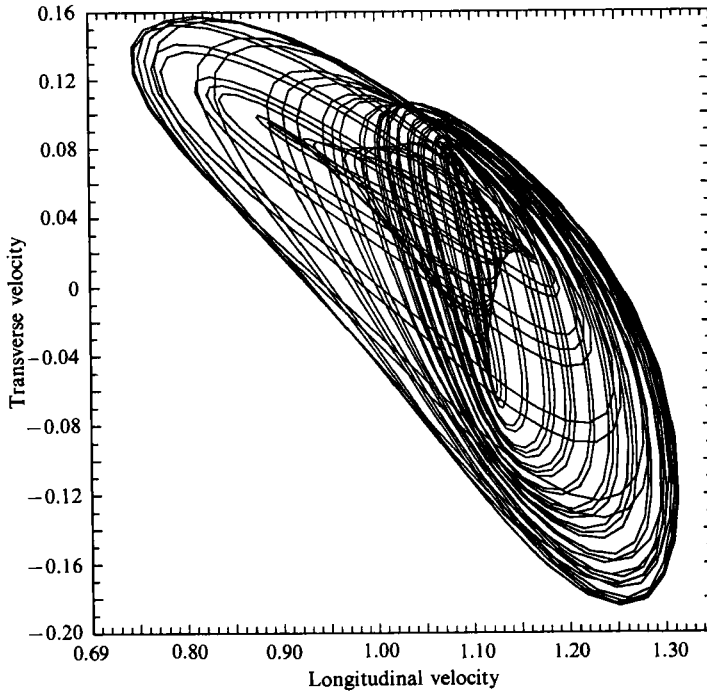
FIGURE 7. Phase diagram of non-lock-in state (intermediate zone), the velocities are measured at the near-wake point $x = 0.7828$, $y = 0.7828$, other conditions same as in figure 6.
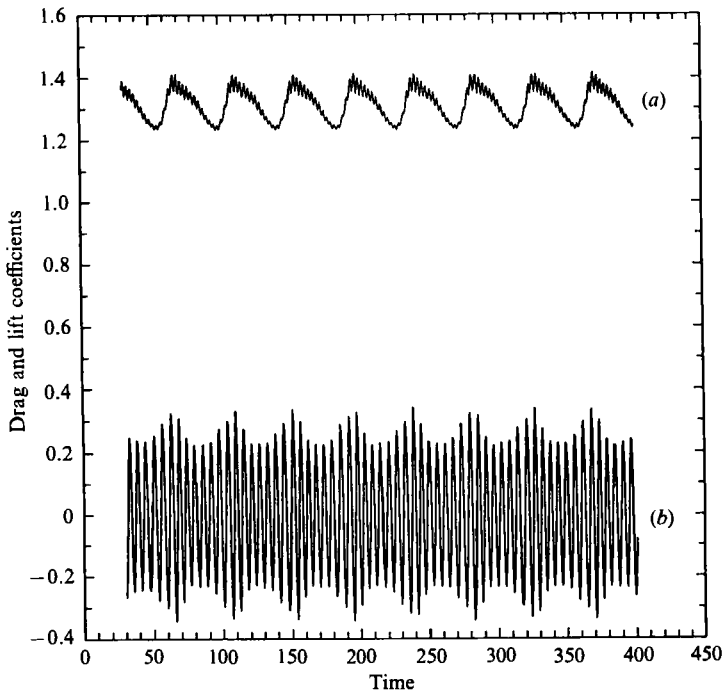

FIGURE 8. Time history of drag (curve a) and lift (curve b) coefficients in non-lock-in state, same conditions as in figure 6.
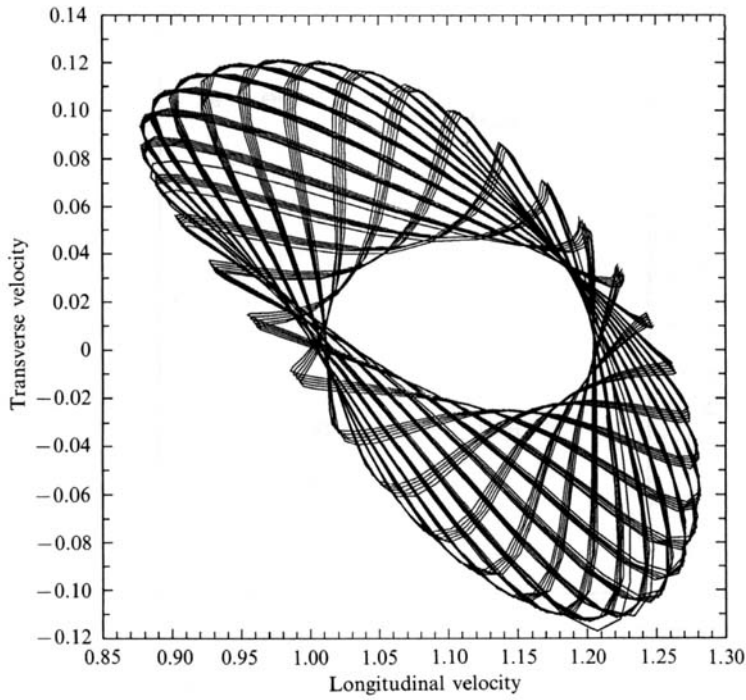
FIGURE 9. Phase diagram for a pure non-lock-in state, velocities are taken at the point $x = 0.7828$, $y = 0.7828$ ($Re = 100$, $A_v = 0.04$ and $f_c = 1.9f_{ns}$). Quasi-periodic characteristics.
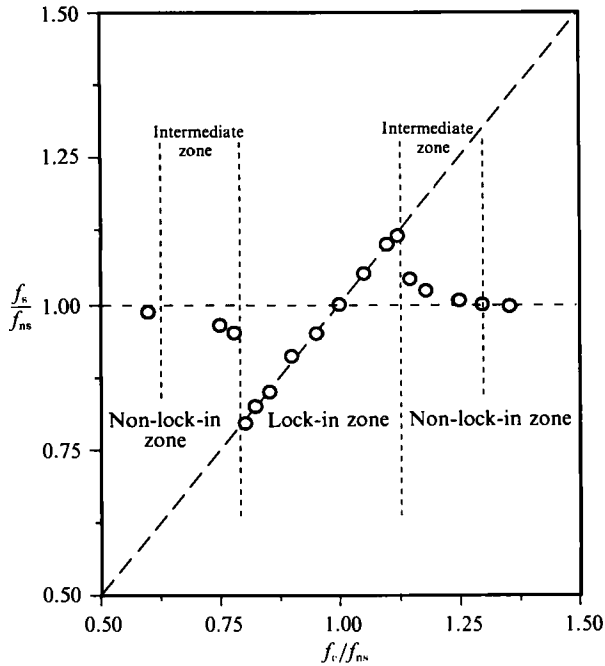

FIGURE 10. Reduced vortex shedding frequency f_s/f_{ns} versus reduced forcing frequency f_c/f_{ns}, $A_v/D = 0.05$ and $Re = 100$.
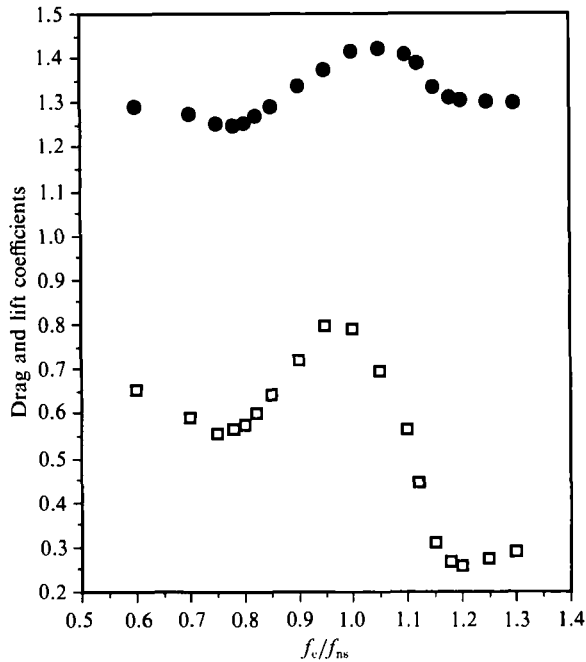
FIGURE 11. Mean drag coefficient and maximum lift coefficient versus reduced driving frequency f_c/f_{ns}, same conditions as in figure 10: ●, mean drag coefficient; □, maximum lift coefficient.

3.2. *Variation of the shedding frequency*

We have shown in the previous section that within the intermediate zone, the vortex shedding frequency is not exactly the Strouhal frequency of a stationary cylinder; it drifts towards the forcing frequency. The variation of reduced shedding frequency f_s/f_{ns} as a function of forcing frequency for a constant velocity vibration amplitude $(A_v/D = 0.05)$ is plotted in figure 10. The shedding frequency is equal to the natural shedding frequency only when the forcing frequency is well below or above the boundary separating the lock-in and the non-lock-in states. In the intermediate non-lock-in range, the measured shedding frequency varies smoothly with the forcing frequency before being locked on to it; i.e., if $f_c < f_{ns}$, the shedding frequency f_s is found to be less than f_{ns}; conversely, if $f_c > f_{ns}$, f_s is greater than f_{ns}. Synchronization is more likely to occur when the forcing frequency approaches the Strouhal frequency from below than from above. The same behaviour can also be found in Koopmann's (1967) experimental data.

3.3. *Amplification of drag and lift coefficients*

Not only the phase diagram shows abrupt changes of trajectory when lock-in occurs; the forces exerted on the cylinder do as well. Based on our results, the variations of drag and lift coefficients with respect to reduced frequency f_c/f_{ns} are plotted in figure 11. Both coefficients are significantly amplified in the lock-in range.

3.4. *Lock-in diagram*

Experimental studies have shown that the range of synchronization depends on amplitude and Reynolds number (e.g. Bishop & Hassan 1964; Koopmann 1967). An increase in amplitude or a decrease in Reynolds number leads to an increase in the lock-in range. Quantitative determination of the exact range of synchronization as
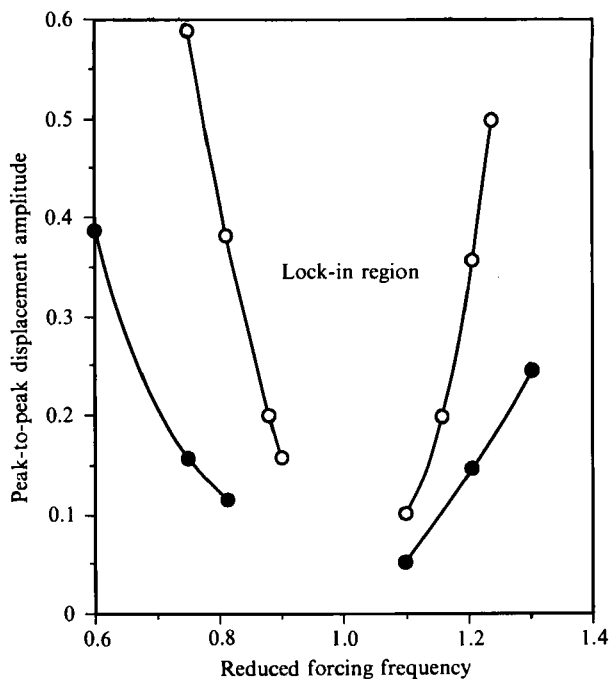
FIGURE 12. Lock-in diagram for Re = 100: ○, Koopman's experimental data; ●, present numerical simulation.

functions of both Reynolds number and vibration amplitude is extremely time consuming, requiring a large amount of computation. Therefore, only the influence of amplitude was explored in the present study. The boundary frequencies are determined by power spectra and phase diagram analysis. If the dominant frequency equals the forcing frequency and its corresponding Lissajous figure exhibits a one-loop trajectory, we say that the lock-in state has been reached. By continuously changing the forcing frequency, boundary frequencies at different vibration amplitudes can be readily derived.

Based on our numerical results, a quantitative diagram of the lock-in range is drawn in figure 12 for Re = 100. Compared with Koopmann's experimental data (for a virtually vibrating cylinder), our prediction has the same trend of variation, but overestimates the range of synchronization. This is possibly because we used a parietal forcing mechanism instead of real cylinder oscillation. In addition, this difference can also be attributed to the possible tridimensional effect, and/or aeroelastic mode selection effect existing in experiments, not included in the present two-dimensional model.

4. Results for a cylinder oscillating in the wake of an upstream cylinder

In §3, we discussed the response modes of a circular cylinder oscillating in uniform flows. However, upstream wake–structure–downstream wake interactions are often observed in arrays of tubes in heat exchangers, in power lines and in conductor bundles. Obviously, such a system is much more complex than that of a single cylinder, since its response state depends not only on the forced vibration of the cylinder but also on the non-uniformity of the oncoming flow as well as the unsteadiness of its own wake. In this section, the response states of an oscillating
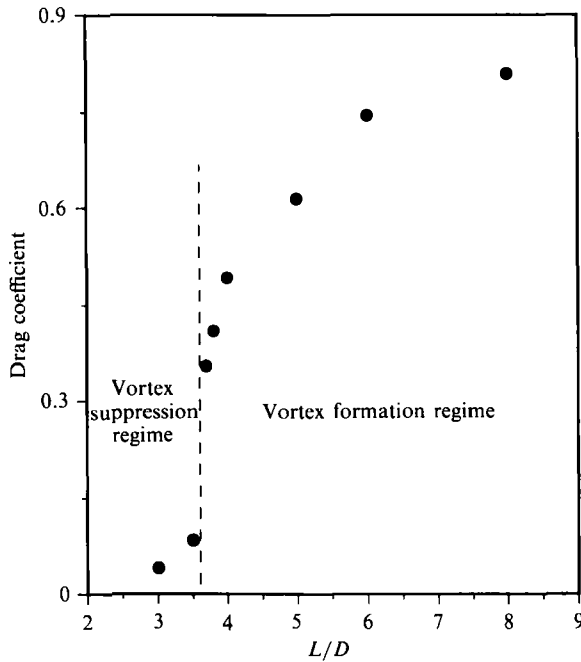
FIGURE 13. Mean drag coefficient of the downstream cylinder versus cylinder spacings of two cylinder in tandem (cylinders are fixed). We notice two distinct flow regimes: vortex suppression regime (VS regime) and the vortex formation regime (VF regime).

cylinder in the wake of an upstream cylinder are discussed. The two cylinders are in a tandem arrangement (with the upstream cylinder at rest), they have the same radius D and are separated by the distance L. The parameter $A_v/2\pi f_c$ is kept constant (corresponding to fictitious displacement amplitude $A = 0.14$) in order to compare with the existing experimental data. Computations are performed for three different spacings $(L/D = 3, 4$ and $6)$.

4.1. *Different flow configurations at different spacings*

The complexity of flow interference for two cylinders in tandem has been demonstrated in previous investigations for fixed cylinders. Here we recall briefly the vortex shedding characteristics in the absence of external forcing (Zdravkovich 1977; Li 1989; Li *et al.* 1991). Basically, there are two different flow patterns. At small cylinder spacing, because of the presence of downstream cylinder the shear layers separating from the upstream cylinder reattach to the downstream cylinder. As a consequence, the formation of a vortex street between the cylinders is inhibited. We refer to this regime as the 'vortex suppression regime' (VS regime). In this flow configuration, the oncoming flow to the downstream cylinder is very weak and leads to an equally weak vortex street behind the downstream cylinder. In some cases, there is even no vortex shedding occurring (at least in the near wake). But it is possible that the formation of the classic Bénard–von–Kármán vortex street occur further downstream, outside the computational region; however, there are no available experimental observations. Conversely, at large spacings, the vortex street behind the upstream cylinder has sufficient room to develop. The oncoming flow becomes strong both in transverse oscillation and in intensity, leading to an even stronger vortex street behind the downstream cylinder. We refer to this regime as the
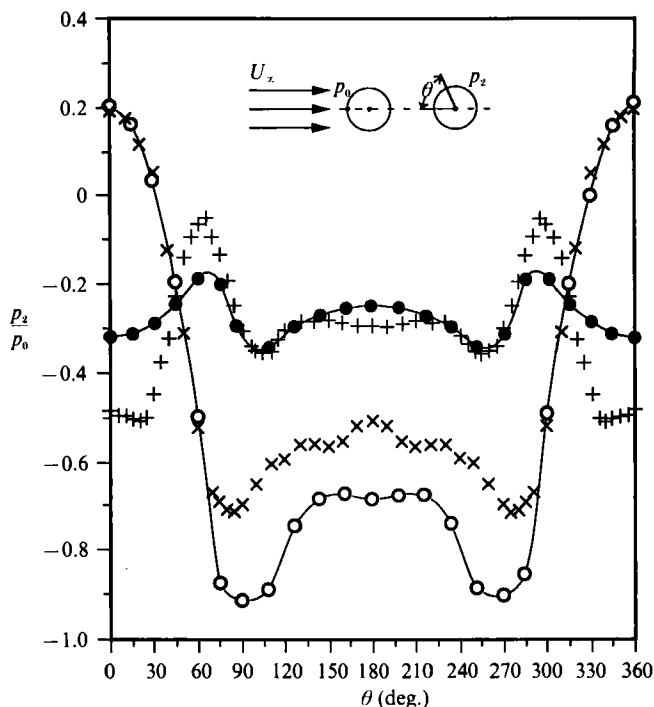
FIGURE 14. The averaged pressure distribution (normalized by the stagnant pressure of the upstream cylinder) around the downstream cylinder for the two different flow regimes. VF regime: ○, present numerical simulation ($L/D = 6$, $Re = 80$); ×, Ishigai *et al.*'s experiments ($L/D = 5$, $Re = 3900$). VS regime: ●, present work ($L/D = 3$, $Re = 80$); +, Ishigai *et al.*'s experiments ($L/D = 3$, $Re = 3900$).

'vortex formation regime' (VF regime). Between the two regimes, there is no distinct transition regime. The abrupt change from one flow pattern to the other is clearly demonstrated in figure 13, showing a sudden jump (at $L/D \approx 3.7$) in the drag coefficient of the downstream cylinder as a function of cylinder spacing: two distinct zones are easily identified. The two different flow regimes can also be distinguished by computing or measuring the time-averaged circumferential pressure distribution on the downstream cylinder. In the VF regime, there is only one peak in the pressure distribution plot (at $\theta = 0$, see figure 14), corresponding to the front stagnant point. This is similar to the circumferential pressure curve of the upstream cylinder, indicating that flow structures are similar for both cylinders. However, in the VS regime, the pressure distribution on the downstream cylinder is quite different from that on the upstream cylinder; the former has two peaks related to the two reattachment points of the upstream shear layers (at $\theta = 70$ and 290 respectively, figure 14). This reattachment prevents the formation of a vortex street behind the upstream cylinder and, makes the two-cylinder system a streamline-like body which discourages the vortex formation and weakens the vortex shedding strength behind the downstream cylinder. The comparison between our numerical results and Ishigai *et al.*'s experimental data (figure 14) shows qualitatively similar variations. The large Reynolds number difference ($Re = 80$ in the numerical simulation and $Re = 3900$ in the experiment) does not affect the pressure distribution characteristics much, which implies that the flow configuration (and thus the flow regime) is the determinating factor of the problem.
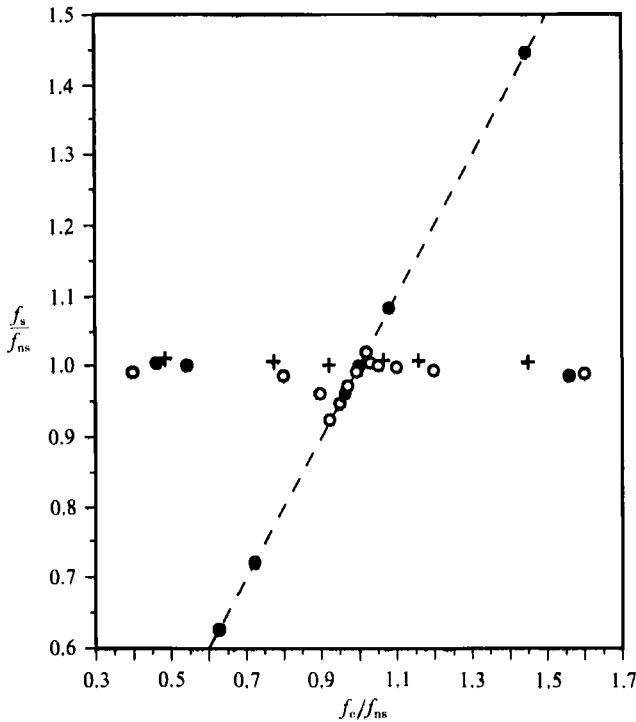
　　　　　　　　　　J. Li, J. Sun and B. Roux

FIGURE 15. Reduced shedding frequency f_s/f_{ns} of the downstream cylinder as a function of reduced driving frequence f_c/f_{ns} for different spacings: $L/D = 3$ (●), 4 (○) and 6 (+), $A = 0.14$ and $Re = 80$. The natural shedding frequencies at three spacings are different, $f_{ns} = 0.1198$ for $L/D = 3$; $f_{ns} = 0.1440$ for $L/D = 4$; and $f_{ns} = 0.1490$ for $L/D = 6$.

Spacing between the cylinders L/D	Lock-in zone	
	Tanida *et al.* (1973)	Present work
3	0.075–0.180	0.07–0.183
4	0.075–0.160	0.133–0.147
5 (Tanida *et al.*)	No clear lock-in	No clear lock-in
6 (present work)	is detected	is detected

TABLE 2. Comparison of the lock-in range with Tanida *et al.*'s data for a circular cylinder oscillating in the wake of another cylinder ($Re = 80$, $A = 0.14$)

4.2. *The effects of oncoming flow oscillation on the response states of the oscillating cylinder wake*

Now let us consider the case where the downstream cylinder is forced to oscillate transversely. When the cylinder spacing is small, both the upstream cylinder wake and the downstream one are very weak, the finite-amplitude oscillation of parietal velocity of the second cylinder becomes comparatively important, and the vortex shedding behind the second cylinder is more apt to synchronize with the driving frequency since its oncoming flow is too weak to affect its response state. In the opposite case, i.e. when the spacing is large, because of the establishment of a vortex street behind the upstream cylinder, the oscillation of downstream cylinder's oncoming flow becomes fairly strong compared to the cylinder vibration itself, and
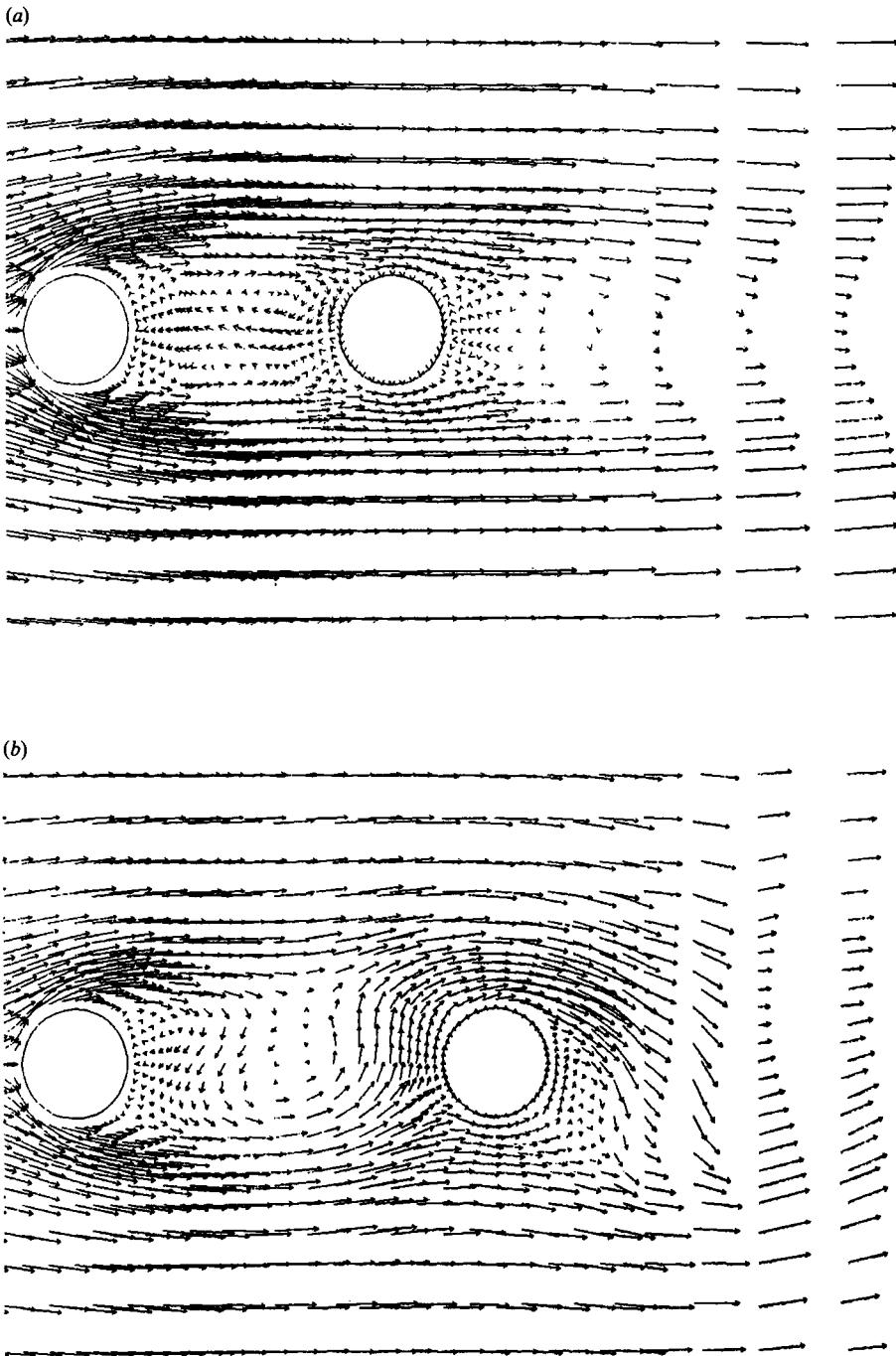
(a)

(b)

FIGURE 16. Velocity fields of two cylinders in a tandem arrangement, downstream cylinder oscillating transversely, upstream cylinder fixed at $Re = 80$. (a) for $L/D = 3$, lock-in state, the vortex wakes behind both of the cylinders are quite weak. Conversely, for (b) $L/D = 4$, non-lock-in state, the development of periodic vortex streets is recovered.
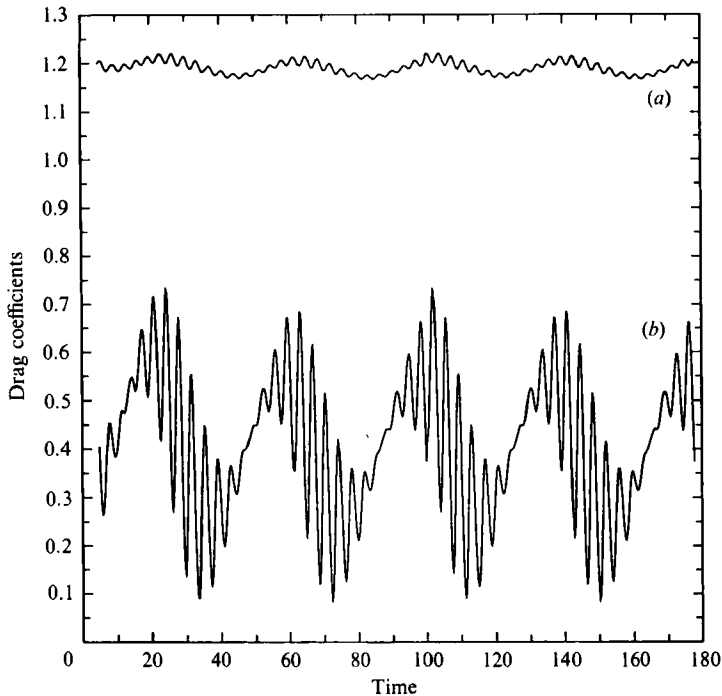
FIGURE 17. Time signals of the drag coefficients at $L/D = 4$, $f_c = 1.1f_{ns}$, $A = 0.14$ and $Re = 80$: (a) upstream cylinder; (b) downstream cylinder.

it completely dominates the flow and controls the vortex shedding from the downstream cylinder. The farther downstream the cylinder is placed, the stronger is its oncoming flow and the more difficult it is for synchronization with the cylinder vibration to take place, except for when the driving frequency is very close to the shedding frequency and the driving forces are sufficiently strong.

These arguments are completely confirmed by our numerical results. The lock-in diagram at different spacings is displayed in figure 15. A considerably larger lock-in range is detected in the VS regime $(L/D = 3)$ but a rather small or even indistinguishable lock-in range is found in the VF regime for $L/D = 4$ and 6, respectively. A comparison between our numerical results and Tanida et al.'s experimental data is given in table 2. Good agreement is obtained for the lock-in range except for the critical spacing value. Tanida et al. reported that the sudden change in flow pattern occurred at $L/D = 5$, while in our simulation, this value is 3.7.

Flow fields characteristic of the two flow regimes are shown in figure 16. In the VS regime, the upstream cylinder wake is almost stagnant, containing two recirculation regions attached to the downstream cylinder surface. The oscillation of the downstream cylinder wake is fairly weak. However, in the VF regime, vortices are shed periodically from both upstream and downstream cylinders.

The nonlinear interactions among the oncoming flow, cylinder vibration and its vortex wake are apparently seen in time histories of drag and lift coefficients plotted in figures 17 and 18, showing similar characteristics to those we have observed in the single oscillating cylinder case. Not only does the downstream cylinder exhibits combined wave forms but so does the upstream cylinder. This indicates that the forcing wave is transferred in both the upstream and downstream directions. Though at large spacings the forcing wave is negligible compared to the oncoming wave, it
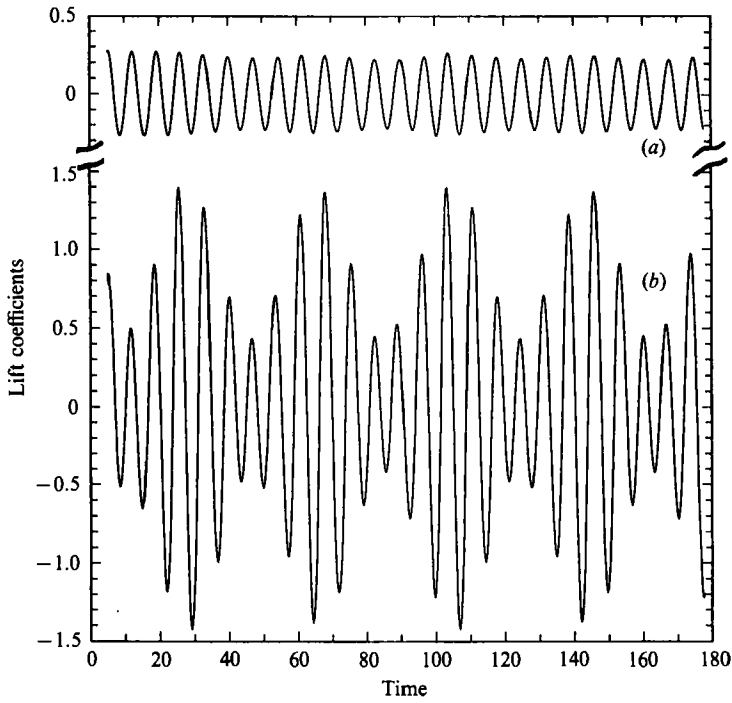
FIGURE 18. Time evolution of lift coefficients, same conditions as figure 17: (*a*) upstream cylinder; (*b*) downstream cylinder.
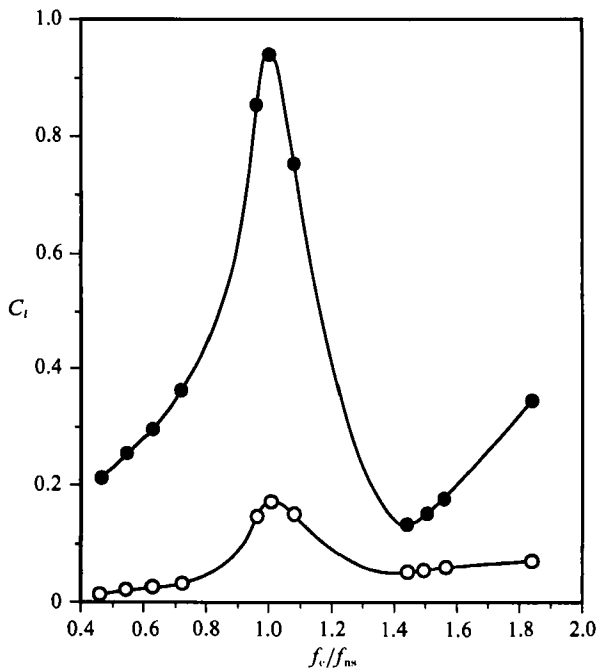

FIGURE 19. Maximum lift coefficients as a function of the reduced driving frequency f_c/f_{ns}, for $L/D = 4$, $A = 0.14$ and $Re = 80$: $\bigcirc$, upstream cylinder; $\bullet$, downstream cylinder.
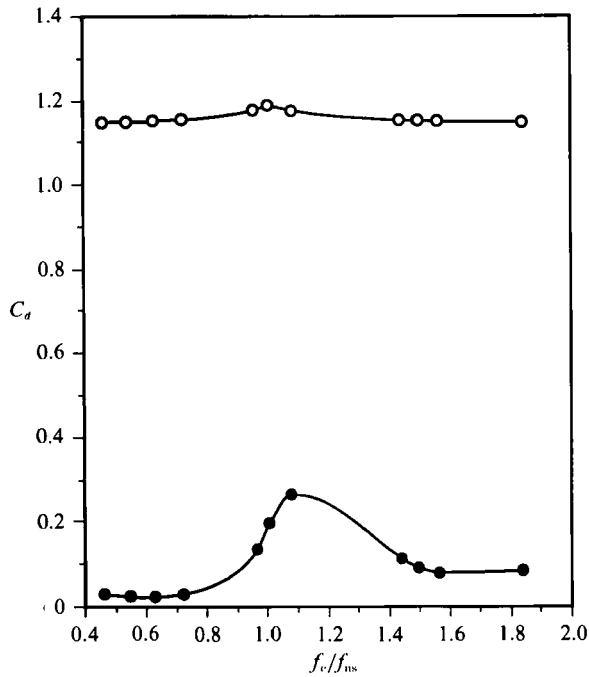
FIGURE 20. Mean drag coefficients versus reduced driving frequency f_c/f_{ns}, same conditions as in figure 19: ○, upstream cylinder; ●, downstream cylinder.

can still make its presence felt through nonlinear effects. The downstream cylinder has lower mean drag but greater lift due to the influence of the upstream cylinder wake. These interactions are more pronounced for small spacings. In the lock-in state, the upstream cylinder wake is also synchronized to the driving frequency. Another aspect of this nonlinear effect is to increase the lift force on the upstream cylinder (figure 19). However, little influence is found on the drag force (figure 20). For the downstream cylinder, both the drag and lift coefficients are greatly amplified in the lock-in region, showing the presence of a stronger wake compared to our single-cylinder observations.

We have demonstrated in the above results that, in the case of two cylinders in tandem, the response state of the wake is largely dominated by the flow configuration. Though this study deals with a transversely vibrating cylinder case, it can be predicted that when the downstream cylinder is forced to oscillate in the flow direction, similar characteristics of the response state will be found, except that in this case the principal lock-in region will be around $2f_{ns}$ instead of f_{ns} (since it is the longitudinal fluctuation component in the upstream cylinder wake that will be responsible for synchronization). In the general case, where the downstream cylinder is allowed to oscillate in an arbitrary direction, lock-in around f_{ns} and $2f_{ns}$ will coexist. How the two lock-in ranges vary with the oscillation angle, whether a common lock-in can be formed, and what is the influence of intercylinder spacing, etc. are interesting questions. This problem is currently under investigation and we hope that we will be able to answer these questions.

5. Conclusion

The two-dimensional coupling system containing a vibrating cylinder and its oscillatory wake has been numerically investigated in this study. The response states of one circular cylinder oscillating in uniform flow or in the wake of an upstream cylinder are classified as a lock-in state and a non-lock-in state, functions of both forcing frequency and excitation amplitude.

For given amplitude, the response modes of the cylinder wake can be either periodic or quasi-periodic. In the lock-in state, only the periodic mode is observed in the wake where the vortex shedding is controlled by the external forcing on the cylinder. In the non-lock-in state, quasi-periodic modes are identified, the forced oscillation of the cylinder and that of its own wake become comparatively important and, therefore, the two modes coexist in the wake, showing composite wave forms in time history of drag, lift and velocity variation and two distinct peaks as well as their harmonics in power spectra. The chaotic state found in the numerical simulations of Karniadakis & Triantafyllou was not observed in the present study. However, the forcing mechanism is different in our case, therefore whether a chaotic state can be found under such forcing condition is not certain. Also, the region in which a chaotic state is observed in Karniadakis & Triantafyllou's simulation is very narrow, and we made only a few calculations long enough to distinguish the chaotic state; thus the forcing frequencies we used were possibly not located inside the chaotic zone. In the intermediate zone, just outside the lock-in region, the shedding frequency shifted towards the driving frequency. The width of the lock-in region is amplitude dependent: the bigger the forcing amplitude is, the larger the lock-in region becomes. The comparison with the experimental results of Koopmann showed qualitatively good agreement.

The response of a circular cylinder oscillating in the wake of an upstream is strongly influenced by the oscillation of its oncoming flow. This is in fact caused by the abrupt change of flow regimes. It is found that in the vortex suppression regime, the oncoming flow is weak, thus the synchronization of the cylinder wake with the forcing frequency is more likely to occur and a large lock-in zone is obtained. On the other hand, in the vortex formation regime, the intensity of the driving force is so weak compared with that of the oncoming oscillatory flow that the synchronization can hardly occur. These results agree well with Tanida *et al.*'s experimental data.

REFERENCES

ANAGNOSTOPOULOS, P. 1989 Numerical solution for laminar two-dimensional flow about a fixed and transversely oscillating cylinder in a uniform stream. *J. Comput. Phys.* **85**, 434.

BARBI, C., FAVIER, D. P., MARESCA, C. A. & TELIONIS, D. P. 1986 Vortex shedding and lock-on of a circular cylinder in oscillatory flow. *J. Fluid Mech.* **170**, 572.

BEARMAN, P. W. 1984 Vortex shedding from oscillating bluff bodies. *Ann. Rev. Fluid Mech.* **16**, 195.

BERGER, E. & WILLE, R. 1972 Periodic flow phenomena. *Ann. Rev. Fluid Mech.* **4**, 313.

BISHOP, R. E. D. & HASSAN, A. Y. 1964 The lift and drag forces on a circular cylinder oscillating in a flowing fluid. *Proc. R. Soc. Lond.* A **227**, 51.

BLEVINS, R. D. 1977 *Flow Induced Vibrations*. Van Nostrand Reinhold.

BRAZA, M., CHASSAING, P. & HA MINH, H. 1986 Numerical study and physical analysis of the pressure and velocity fields in the near wake of a circular cylinder. *J. Fluid Mech.* **165**, 79.

CHILUKURI, R. 1987 Incompressible laminar flow past a transversely vibrating cylinder. *Trans. ASME*, I: *J. Fluids Engng* **109**, 166.

ENGELMAN, M. S. & JAMNIA, M. A. 1990 Transient flow past a circular cylinder: a benchmark solution. *Intl J. Numer. Methods Fluids.* **11**, 985.

GASTER, M. 1969 Vortex shedding from slender cones at low Reynolds numbers. *J. Fluid Mech.* **38**, 565.

GASTER, M. 1971 Vortex shedding from circular cylinders at low Reynolds numbers. *J. Fluid Mech.* **46**, 749.

GRIFFIN, O. M. & RAMBERGE, S. E. 1975 On vortex strength and drag in bluff-body wakes. *J. Fluid Mech.* **69**, 721.

ISHIGAI, S., NISHIKAWA, E., NISHIMURA, K. & CHO, K. 1972 Experimental study on structure of gas flow in tube banks with tube axes normal to flow (part 1, Karman vortex flow around two tubes at various spacings). *Bull. JSME* **15**, No. 86, 949.

KARNIADAKIS, G. E. & TRIANTAFYLLOU, G. S. 1989 Frequency selection and asymptotic states in laminar wakes. *J. Fluid Mech.* **199**, 441.

KOOPMANN, G. H. 1967 The vortex wakes of vibrating cylinders at low Reynolds numbers. *J. Fluid Mech.* **28**, 501.

LI, J. 1989 Bi-dimensional simulation of flow past one and two cylinders in tandem arrangement using finite element method. PhD Dissertation. University of Aix-Marseille I (in French).

LI, J., CHAMBAREL, A., DONNEAUD, M. C. & MARTIN, R. 1991 Numerical study of laminar flow past one and two circular cylinders. *Computers & Fluids* **19**, 155.

SREENIVASAN, K. R. 1985 Transition and turbulence in fluid flows and low-dimensional chaos. In *Frontiers in Fluid Mechanics* (ed. S. H. Davis & J. L. Lumley), p. 41. Springer.

TANIDA, Y., OKAJIMA, A. & WATANABE, Y. 1973 Stability of a circular cylinder oscillating in uniform flow or in a wake. *J. Fluid Mech.* **61**, 769.

TRITTON, D. J. 1959 Experiments on the flow past a circular cylinder at low Reynolds numbers. *J. Fluid Mech.* **6**, 547.

TRITTON, D. J. 1971 A note on vortex streets behind circular cylinders at low Reynolds numbers. *J. Fluid Mech.* **45**, 203.

VAN ATTA, C. W. & GHARIB, M. 1987 Ordered and chaotic vortex streets behind circular cylinders at low Reynolds numbers. *J. Fluid Mech.* **174**, 113.

WILLIAMSON, C. H. K. 1989 Oblique and parallel modes of vortex shedding in the wake of a circular cylinder at low Reynolds numbers. *J. Fluid Mech.* **206**, 579.

ZDRAVKOVICH, M. M. 1977 Review of flow interference between two cylinders in various arrangements. *Trans. ASME*, I: *J. Fluids Engng.* **99**, 618.